

Field variation and mathematics of blowup (場の変分構造と爆発の数理)

Norikazu Saito* (齊藤宣一・富山大人間発達科学部)
Takashi Suzuki† (鈴木貴・阪大基礎工)

1 Introduction

Our purpose is to summarize recently proposed numerical methods concerning simplified system of chemotaxis [7, 6] and is to examine their validity. A typical example of such system is

$$\begin{cases} u_t = \nabla \cdot (\nabla u - u \nabla v) & \text{in } \Omega \times (0, T) \\ -\Delta v = u - \frac{1}{|\Omega|} \int_{\Omega} u & \text{in } \Omega \times (0, T) \\ \frac{\partial u}{\partial \nu} - u \frac{\partial v}{\partial \nu} = \frac{\partial v}{\partial \nu} = 0 & \text{on } \partial\Omega \times (0, T) \\ u|_{t=0} = u_0 & \text{on } \bar{\Omega}, \end{cases} \quad (1)$$

where $u = u(x, t)$, $v = v(x, t)$ are unknown functions of $(x, t) \in \bar{\Omega} \times [0, T)$, $\Omega \subset \mathbb{R}^d$ ($d = 1, 2, 3$) is a bounded domain with the boundary $\partial\Omega$ usually supposed to be smooth, ν is the outer unit normal vector to $\partial\Omega$, and $u_0 = u_0(x) \geq 0, \neq 0$ is a given function defined on $\bar{\Omega}$. This system describes aggregation of cellular slime molds resulting from their chemotactic features, and u and v denote the density of cellular slime molds and the concentration of chemical substance, respectively, whereby the diffusion of u is supposed to be much faster than that of v .

In more detail, the first equation stands for mass conservation and the flux $j = -\nabla u + u \nabla v$ of u is composed of the terms of diffusion and chemotaxis indicated by $-\nabla u$ and $u \nabla v$, respectively, using phenomenological relation. The second equation, on the other hand, describes the formation of the field distribution v by the particle density u . Henceforth, this law is referred to as $v = (-\Delta_{JL})^{-1}u$, where

$$-\Delta v = u - \frac{1}{|\Omega|} \int_{\Omega} u \text{ in } \Omega, \quad \frac{\partial v}{\partial \nu} \Big|_{\partial\Omega} = 0, \quad \int_{\Omega} v = 0.$$

Actually, system (1) is a combination of the Smoluchowski-Poisson equations describing mean field motion of many self-gravitating particles [10]. The classical

*Faculty of Human Development, University of Toyama, Gofuku 3190, Toyamashi 930-8555, Japan

†Division of Mathematical Science, Department of System Innovation, Graduate School of Engineering Science, Osaka University, Machikaneyamacho 1-3, Toyonakashi, 650-8531, Japan, suzuki@sigmath.es.osaka-u.ac.jp

microscopic modelling adopts the Kramers-Moyal expansion [8], while the other derivation uses the renormalized master equation [5] or the kinetic theory [3]. In any case, this system is consistent to the second law of thermodynamics, i.e., mass conservation

$$\|u(\cdot, t)\|_{L^1(\Omega)} = \|u_0\|_{L^1(\Omega)}$$

and the decrease of Helmholtz' free energy

$$\frac{d}{dt}\mathcal{F}(u(\cdot, t)) \leq 0 \quad t \in [0, T), \quad (2)$$

where

$$\mathcal{F}(u) = \int_{\Omega} (u \log u - u) - \frac{1}{2} \langle (-\Delta)_{JL}^{-1}(u), u \rangle$$

with the duality pairing $\langle \cdot, \cdot \rangle$ identified with the L^2 -inner product.

This is not surprising because (1) is the model (B) equation [10] formulated by this free energy:

$$u_t = \nabla \cdot (u \nabla \delta \mathcal{F}(u)), \quad u \frac{\partial}{\partial \nu} \delta \mathcal{F}(u) \Big|_{\partial \Omega} = 0,$$

where $\delta \mathcal{F}(u)$ defined by

$$\frac{d}{ds} \mathcal{F}(u + sw) \Big|_{s=0} = \langle \delta \mathcal{F}(u), w \rangle$$

is identified with $\log u - (-\Delta_{JL})^{-1}u$. Then, we obtain the formation of collapse with quantized mass [9], where $T = T_{\max} \in (0, +\infty]$ denotes the blowup time.

Theorem 1.1. *If $d = 2$ and $T_{\max} < +\infty$, then it holds that*

$$u(x, t) dx \rightarrow \sum_{x_0 \in \mathcal{S}} m_*(x_0) \delta_{x_0}(dx) + f(x) dx$$

as $t \uparrow T = T_{\max}$ in $\mathcal{M}(\overline{\Omega})$, where \mathcal{S} is the blowup set,

$$m_*(x_0) = \begin{cases} 8\pi & (x_0 \in \Omega) \\ 4\pi & (x_0 \in \partial \Omega), \end{cases}$$

and $0 \leq f = f(x) \in L^1(\Omega) \cap C(\overline{\Omega} \setminus \mathcal{S})$.

Study of such profiles of the solution has a long history [9], but the structures of dual variation and scaling invariance are fundamental tools and motivations. Although we have not examined all possibilities, there is also *emergence*. More precisely, local free energy gets to $+\infty$ inside the blowup envelope. Still there are several open problems and recent developments [10].

Meanwhile we have tried to realize these profiles in numerical computation. In this respect, it seems to be reasonable to reproduce the properties of mass conservation and free energy decreasing in the numerical scheme, and first, we shall describe such trials. Thus, in §2, we propose a time discretization provided with a discrete version of (2), and then we consider a finite difference scheme which satisfies the total mass conservation also (§3). In §4, an application to tumor angiogenesis model is presented, and in §5, finite element method is also examined.

However, the fundamental question, what to extent we can believe the simulation, is still open. This will be discussed in the final section.

2 Time discretization

First observation is that the free energy $\mathcal{F}(u)$ is a difference of two functionals,

$$I(u) = \int_{\Omega} u(\log u - 1) \quad \text{and} \quad K(u) = \frac{1}{2} \langle (-\Delta_{JL})^{-1} u, u \rangle,$$

realized as proper, lower semi-continuous, convex functionals in $X = H^1(\Omega)$, provided with the domains $D(I) = \{u \in X \mid u \geq 0, I(u) < +\infty\}$ and $D(K) = X$. From this structure, combining backward and forward schemes to I and K guarantees the decreasing of \mathcal{F} for the discretized solution in time. Henceforth, we adopt the irregular mesh because we are dealing with the blowup phenomena. Thus, taking positive constants τ_1, τ_2, \dots , we put

$$t_n = \tau_1 + \dots + \tau_n \quad (3)$$

and consider the time discrete scheme: Find $\{u^n\}_{n \geq 0}$ such that

$$\begin{cases} \frac{u^n - u^{n-1}}{\tau_n} = \nabla \cdot u^n \nabla (I'(u^n) - K'(u^{n-1})) & \text{in } \Omega \\ u^n \nabla (I'(u^n) - K'(u^{n-1})) \cdot \nu = 0 & \text{on } \partial\Omega. \end{cases} \quad (4)$$

Remark 2.1. Each step of the approximate solution u^n becomes regular so that the sub-differentials $\partial I(u^n)$ and $\partial K(u^{n-1})$ are single-valued and identified with regular functions denoted by $I'(u^n)$ and $K'(u^{n-1})$, respectively.

Theorem 2.1. *If $u^n, u^{n-1} \in X$ satisfy (4), then*

$$\frac{1}{\tau_n} [\mathcal{F}(u^n) - \mathcal{F}(u^{n-1})] \leq 0. \quad (5)$$

Proof. Since I' and $-K'$ are convex, it holds that

$$\mathcal{F}(u) - \mathcal{F}(\hat{u}) \leq \langle I'(u) - K'(\hat{u}), u - \hat{u} \rangle, \quad (u, \hat{u} \in X),$$

and therefore;

$$\begin{aligned} & \mathcal{F}(u^n) - \mathcal{F}(u^{n-1}) \\ & \leq \tau_n \int_{\Omega} (I'(u^n) - K'(u^{n-1})) [\nabla \cdot u^n \nabla (I'(u^n) - K'(u^{n-1}))] \\ & = -\tau_n \int_{\Omega} u^n |\nabla (I'(u^n) - K'(u^{n-1}))|^2 \leq 0. \end{aligned}$$

This leads to (5). □

System (4) may be written as

$$\begin{cases} \frac{u^n - u^{n-1}}{\tau_n} = \nabla \cdot (\nabla u^n - u^n \nabla (Gu^{n-1})) & \text{in } \Omega \\ (\nabla u^n - u^n \nabla (Gu^{n-1})) \cdot \nu = 0 & \text{on } \partial\Omega, \end{cases} \quad (6)$$

for $G = (-\Delta_{JL})^{-1}$, or equivalently,

$$\begin{cases} \frac{u^n - u^{n-1}}{\tau_n} = \nabla \cdot (\nabla u^n - u^n \nabla v^{n-1}) & \text{in } \Omega \\ -\Delta v^{n-1} = u^{n-1} - \frac{1}{|\Omega|} \int_{\Omega} u^{n-1} & \text{in } \Omega \\ \frac{\partial u^n}{\partial \nu} - u^n \frac{\partial v^{n-1}}{\partial \nu} = \frac{\partial v^{n-1}}{\partial \nu} = 0 & \text{on } \partial\Omega. \end{cases} \quad (7)$$

This is a linear elliptic equation of u^n , and its numerical implementation is easy. Actually, this type of time discretization has been often adopted. For instance, it preserves nonincreases of the number of peaks of solutions to parabolic equations for $d = 1$ ([11]). To our knowledge, however, no emphasis on (5) has been made by now.

3 Space discretization: Upwind FDM

To describe the idea and numerical simulations in detail, we shall concentrate on the one dimensional problem with a slightly different field formation law, i.e.,

$$\begin{cases} u_t = (u_x - \mu uv_x)_x & (0 < x < 1, 0 < t < T) \\ 0 = v_{xx} - v + u & (0 < x < 1, 0 < t < T) \\ (u_x - \mu uv_x)|_{x=0,1} = 0 & (0 < t < T) \\ v_x|_{x=0,1} = 0 & (0 < t < T) \\ u(x, 0) = u_0(x) \geq 0, \neq 0 & (0 \leq x \leq 1), \end{cases} \quad (8)$$

where $\mu > 0$ is a constant. Nothing changes in Theorem 1.1 even in this system if $d = 2$. First, we use time discretization defined by (7) and (3), and take $h = 1/N$, where N is a positive integer. Next, we introduce two kinds of mesh points over $(0, 1)$ as

$$x_j = \left(j - \frac{1}{2}\right)h \quad \text{and} \quad \hat{x}_j = jh \quad (j = 1, \dots, N),$$

treating virtual mesh points $x_0 = -h/2$, $x_{N+1} = (N + 1/2)h$, $\hat{x}_{-1} = -h$, and $\hat{x}_{N+1} = (N + 1)h$. Then, we find the approximations of $u(\cdot, t_n)$ and $v_x(\cdot, t_n)$ over *main mesh points* $\{x_j\}_{j=1}^N$;

$$u_j^n \approx u(x_j, t_n) \quad \text{and} \quad b_j^n \approx v_x(x_j, t_n),$$

while compute the approximations of $v(\cdot, t_n)$ and $(u_x - uv_x)(\cdot, t_n)$ over the *dual mesh points* indicated by $\{\hat{x}_j\}_{j=0}^N$;

$$v_j^n \approx v(\hat{x}_j, t_n) \quad \text{and} \quad F_j^n \approx (u_x - uv_x)(\hat{x}_j, t_n).$$

More precisely, let $\{u_j^{n-1}\}_{j=1}^N$ be obtained. Then, we define $\{v_j^{n-1}\}_{j=0}^N$ by the standard finite difference scheme, i.e.,

$$-\frac{v_{j-1}^{n-1} - 2v_j^{n-1} + v_{j+1}^{n-1}}{h^2} + v_j^{n-1} = \tilde{u}_j^{n-1} \quad (j = 0, 1, \dots, N) \quad (9)$$

with $v_{-1}^{n-1} = v_1^{n-1}$ and $v_{N+1}^{n-1} = v_{N-1}^{n-1}$, where

$$\bar{u}_j^{n-1} = \begin{cases} u_1^{n-1} & (j = 0) \\ (u_{j+1}^{n-1} + u_j^{n-1})/2 & (j = 1, 2, \dots, N-1) \\ u_N^{n-1} & (j = N). \end{cases}$$

Next, we approximate $v_x(\cdot, t_{n-1})$ by

$$b_j^{n-1} = \frac{v_j^{n-1} - v_{j-1}^{n-1}}{h} \quad (j = 1, 2, \dots, N),$$

and set

$$b_j^{n-1,+} = \max\{0, b_j^{n-1}\}, \quad b_j^{n-1,-} = \max\{0, -b_j^{n-1}\}.$$

Here, we use the method of upwind approximation, observing that u_j^n and u_{j+1}^n are carried into \hat{x}_j by the flows $b_j^{n-1,+}$ and $-b_{j+1}^{n-1,-}$, respectively. In more precise, the approximation F_j^n of the flux $u_x - \mu uv_x$ at (\hat{x}_j, t_n) is defined by

$$F_j^n = \frac{u_{j+1}^n - u_j^n}{h} - \mu b_j^{n-1,+} u_j^n + \mu b_{j+1}^{n-1,-} u_{j+1}^n \quad (j = 1, 2, \dots, N),$$

and thus, our scheme is represented as follows:

$$\frac{u_j^n - u_j^{n-1}}{\tau_n} = \frac{F_j^n - F_{j-1}^n}{h}. \quad (10)$$

This means that

$$\frac{u_j^n - u_j^{n-1}}{\tau_n} = \Delta_h u_j^n - D_h (b_j^{n-1,+} u_j^n) + D_h^* (b_j^{n-1,-} u_j^n), \quad (11)$$

where

$$D_h w_j = \frac{w_j - w_{j-1}}{h}, \quad D_h^* w_j = \frac{w_{j+1} - w_j}{h}, \quad \Delta_h w_j = D_h^* D_h w_j,$$

and the boundary and initial values are prescribed by

$$\begin{cases} F_0^n = \frac{u_1^n - u_0^n}{h} - b_0^{n-1,+} u_0^n + b_1^{n-1,-} u_1^n = 0, \\ F_N^n = \frac{u_{N+1}^n - u_N^n}{h} - b_N^{n-1,+} u_N^n + b_{N+1}^{n-1,-} u_{N+1}^n = 0 \end{cases} \quad (12)$$

and

$$u_j^0 = u_0(x_j) \quad (j = 1, \dots, N), \quad (13)$$

respectively.

This scheme is provided with mass conservation, positivity conservation, and well-posedness [7].

Theorem 3.1. *Relations (10) and (12) imply*

$$\sum_{j=1}^N u_j^n h = \sum_{j=1}^N u_j^{n-1} h. \quad (14)$$

Theorem 3.2. Given $\{u_j^{n-1}\}_{j=1}^N$ satisfying $u_j^{n-1} \geq 0$ for $1 \leq j \leq N$, and take $\tau > 0$ and $\varepsilon \in (0, 1]$. Then, (10) with (12), defined for

$$\tau_n = \min \left\{ \tau, \frac{\varepsilon h}{2b_{\max}^{n-1}} \right\} \quad \text{and} \quad b_{\max}^{n-1} = \max_{1 \leq j \leq N} |b_j^{n-1}|, \quad (15)$$

admits a unique solution $\{u_j^n\}_{j=1}^N$ such that $u_j^n > 0$, where $1 \leq j \leq N$.

Remark 3.1. The a priori estimate

$$0 < \min_{1 \leq j \leq N} u_j^n \leq \max_{1 \leq j \leq N} u_j^n \leq \sum_{j=1}^N u_j^0 \leq \frac{1}{h} \max_{0 \leq x \leq 1} u_0(x)$$

holds and hence $\{u_j^n\}$ never blows up in finite time. In other words, there is a $c_h > 0$ such that $\tau_n > c_h$. Figure 1 shows numerical experiments for several (μ, λ) 's for $\lambda = \|u_0\|_{L^1}$, where highly concentrated solutions are captured.

Remark 3.2. In case that the central difference formula $\tilde{D}_h \varphi_i = (\varphi_{i+1} - \varphi_{i-1})/(2h)$ is employed for the upwind approximation, we obtain

$$\frac{u_i^{n+1} - u_i^n}{\tau_n} = \Delta_h u_i^{n+1} - \tilde{D}_h \{b_i^n u_i^{n+1}\}$$

for (11) with the correspondence of a modified boundary condition. Then, the conditions

$$hb_{\max}^{n-1} \leq 2 \quad \text{and} \quad \tau_n b_{\max}^{n-1} \leq h$$

are required in order to guarantee the conservation of positivity, which, however is unrealistic because we do not know any a priori estimate for b_{\max}^n .

Remark 3.3. The discrete analogue of J is, for example,

$$J_h(u_h^n) = \sum_{j=1}^N (u_j^n \log u_j^n - u_j^n) h - \frac{1}{2} \sum_{j=1}^N \frac{v_{j-1}^n + v_j^n}{2} u_j^n h,$$

where $\{(u_h^n, v_h^n)\}$ denote a solution of (10) and (12). It is natural to expect that

$$\frac{1}{\tau_n} [J_h(u_h^n) - J_h(u_h^{n-1})] \leq 0. \quad (16)$$

However, the previous argument fails in this case, and the numerical result indicates that (16) is not valid if λ and μ are large enough. In Fig. 2, we plot $(t_n, J_h(u_h^n))$ for several (μ, λ) 's. In the case of $(\mu, \lambda) = (1, 1), (1, 50), (1, 100)$, Inequality (16) really takes place. However, in the case of $(\mu, \lambda) = (50, 100)$, we can observe that there is a time interval such that $J_h(u_h^n) > J_h(u_h^{n-1})$ holds there. Lyapunov's property in fully discrete cases has room for further study.

4 Tumor angiogenesis simulation

The above described concept is applicable to the tumor angiogenesis computation [5] in $S^1 = \mathbb{R}/\mathbb{Z}$:

$$\begin{cases} P_t = (P_x - aPW_x)_x & (x \in S^1, 0 < t < T), \\ W_t = P & (x \in S^1, 0 < t < T), \\ P(x, 0) = P_0(x) \geq 0, \neq 0, & (x \in S^1) \\ W(x, 0) = W_0(x). & (x \in S^1). \end{cases} \quad (17)$$

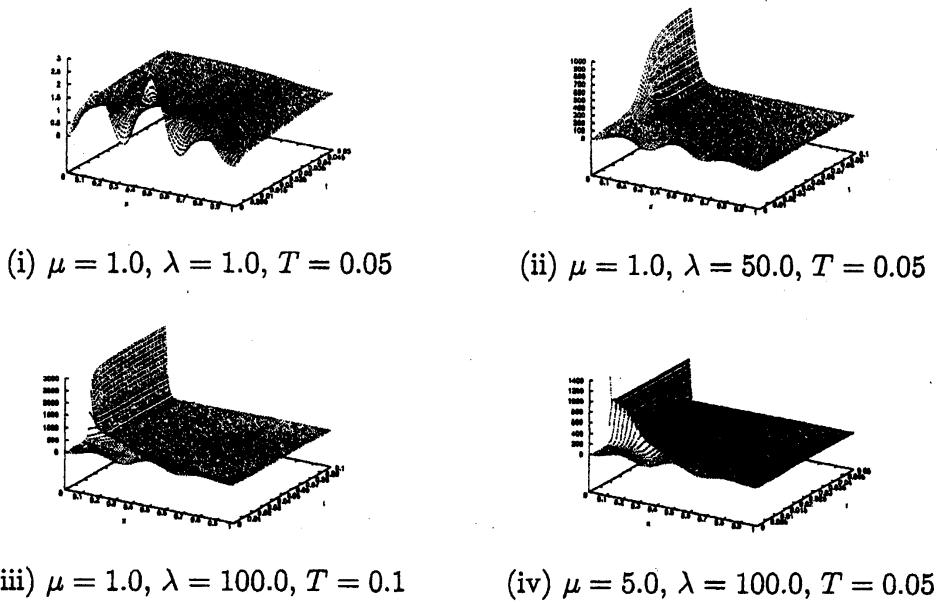


Figure 1: Behavior of numerical solutions for $u(x, t)$ with $\lambda = \|u_0\|_{L^1}$.

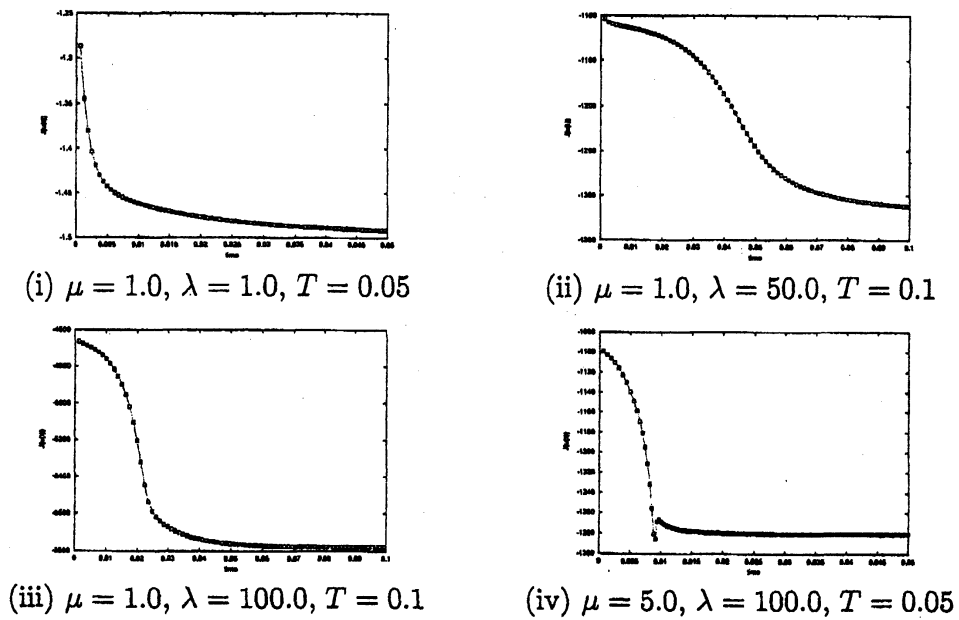


Figure 2: Behavior of $J(u(t))$.

In Fig. 3, we plot numerical solutions to $P(x, t)$ for $a = -1, -50$, $\lambda = \|P_0\|_{L^1(S^1)} = 1, 100$ and $W_0(x) \equiv 0$. There are decaying traveling waves when the effect of chemotaxis is stronger than that of diffusion.

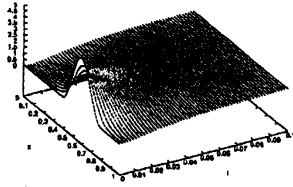
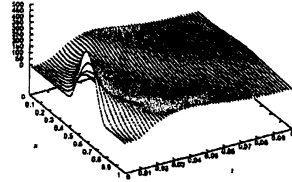
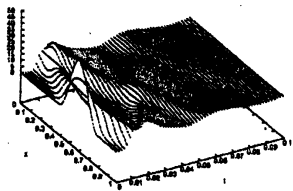
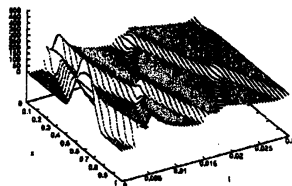
(i) $a = -1.0, \lambda = 1.0, T = 0.1$ (ii) $a = -1.0, \lambda = 100.0, T = 0.1$ (iii) $a = -50.0, \lambda = 10.0, T = 0.1$ (iv) $a = -50.0, \lambda = 100.0, T = 0.03$

Figure 3: Behavior of numerical solutions for $P(x, t)$ with $\lambda = \|P_0\|_{L^1(S^1)}$.

5 Space discretization: Upwind FEM

Finite element method is also applicable to realize our concept [6]. We take the case that $\Omega \subset \mathbb{R}^d$, $d = 2, 3$, is a convex polyhedral domain, noting that mass of collapse formed at the corner of $\partial\Omega$ with the angle $\theta \in (0, 2\pi)$ is equal to 4θ .

First, we take $W^{m,p} = W^{m,p}(\Omega)$, $H^m = W^{m,2}$, $L^p = L^p(\Omega)$, $\|\cdot\|_{m,p} = \|\cdot\|_{W^{m,p}}$, $\|\cdot\|_p = \|\cdot\|_{L^p}$ for $m \in \mathbb{N}$ and $p \in [1, \infty]$. The standard inner product in L^2 is denoted as (\cdot, \cdot) . Then, we put, for $p \in [1, \infty)$,

$$\mathcal{W}_p = \left\{ v \in W^{2,p} \mid \frac{\partial v}{\partial \nu} = 0 \text{ on } \partial\Omega \right\}.$$

Given $f \in L^2$, we define $v \in H^1$ by

$$(\nabla v, \nabla \chi) + (v, \chi) = (f, \chi) \quad \forall \chi \in H^1.$$

Writing $v = Gf$, we obtain $G : L^2 \rightarrow \mathcal{W}_2 \subset L^2$ by the elliptic regularity. We use also the trilinear form b on $L^2 \times H^1 \times H^1$ defined by

$$b(w, u, \chi) = - \int_{\Omega} u \nabla G w \cdot \nabla \chi \, dx \quad (w \in L^2, u \in H^1, \chi \in H^1).$$

Then, it holds that

$$\begin{aligned} |b(w, u, v)| &\leq \|u\|_3 \|\nabla G w\|_6 \|\nabla \chi\|_2 && \text{(Hölder's inequality)} \\ &\leq \|u\|_{1,2} \|\nabla G w\|_{1,2} \|\nabla \chi\|_2 && \text{(Sobolev's inequality)} \\ &\leq \|u\|_{1,2} \|w\|_2 \|\nabla \chi\|_2 && \text{(elliptic regularity)} \end{aligned}$$

for $w \in L^2, u \in H^1, \chi \in H^1$. Although full-weak form derived from the symmetrization is useful in theoretical study [9, 10], semi-weak form is sufficient for our purpose: Find $u \in C^1([0, T] : H^1)$ such that

$$\left(\frac{du(t)}{dt}, \chi \right) + (\nabla u(t), \nabla \chi) + \mu b(u(t), u(t), \chi) = 0, \quad \forall \chi \in H^1, \forall t \in (0, T)$$

$$u(0) = u_0 \in H^1. \quad (18)$$

Let $\{\mathcal{T}_h\} = \{\mathcal{T}_h\}_{h>0}$ be a regular family of triangulations \mathcal{T}_h of Ω : (i) \mathcal{T}_h is a set of closed d -simplices (elements), and $\bar{\Omega} = \bigcup \{J \mid J \in \mathcal{T}_h\}$; (ii) any two elements of \mathcal{T}_h meet only in entire common faces or sides or in vertices; (iii) there exists a positive constant γ_1 such that

$$h_J \leq \gamma_1 \rho_J, \quad \forall J \in \mathcal{T}_h \in \{\mathcal{T}_h\}_h,$$

where $h_J = \text{diam}(J)$ and $\rho_J = \max\{\text{diam}(S) \mid S \text{ is a ball included in } J\}$. Here, we employ $h = \max\{h_J \mid J \in \mathcal{T}_h\}$ as the size parameter. Let $\mathcal{P}_h = \{P_i\}_{i=1}^N$ be the set of all vertices of \mathcal{T}_h , N being a positive integer. Although N depends on h , we shall not explicitly express the dependence. We divide \mathcal{P}_h into two subsets $\{P_i\}_{i=1}^{N_I} \subset \Omega$ and $\{P_{N_I+i}\}_{i=1}^{N_B} \subset \partial\Omega$, where $N = N_I + N_B$. With P_i , we associate a function $\hat{\phi}_i \in C(\bar{\Omega})$ such that $\hat{\phi}_i$ is linear on each $J \in \mathcal{T}_h$ and $\hat{\phi}_i(P_j) = \delta_{ij}$, where δ_{ij} denotes Kronecker's delta. We define as

$$X_h = \text{the vector space spanned by } \{\hat{\phi}_i\}_{i=1}^N$$

and regard it as a closed subspace of H^1 . We also consider space X_h , which is equipped with the topology induced from L^2 , and indicate it using the same symbol X_h . The barycentric domain D_i corresponding to P_i is defined as

$$D_i = \bigcup_{J \in \mathcal{S}_i} \{x \in J \mid \phi_j^J(x) \leq \phi_i^J(x), \quad (P_j \in \mathcal{V}(J), P_j \neq P_i)\},$$

where $\mathcal{S}_i = \{S \in \mathcal{T}_h \mid P_i \in S\}$, $\mathcal{V}(J) = \{P_j \in \mathcal{P}_h \mid P_j \in J\}$, and $\{\phi_i^J\}_{i=1}^{d+1}$ is the barycentric coordinates of J with respect to P_i . Let $\bar{\phi}_i \in L^\infty$ be the characteristic function of D_i . We introduce a Hilbert space $\bar{X}_h \subset L^2$ spanned by $\{\bar{\phi}_i\}_{i=1}^N$. We use the lumping operator $M_h : X_h \rightarrow \bar{X}_h$ defined by

$$M_h v_h = \sum_{i=1}^N v_h(P_i) \bar{\phi}_i, \quad (v_h \in X_h).$$

We put

$$(v_h, \chi_h)_h = (M_h v_h, M_h \chi_h), \quad (v_h, \chi_h \in X_h),$$

whereby $(\cdot, \cdot)_h^{1/2}$ is equivalent to $\|\cdot\|_2$ on X_h . Given $f_h \in X_h$, we define $v_h = G_h f_h \in X_h$ by

$$(\nabla v_h, \nabla \chi_h) + (v_h, \chi_h) = (f_h, \chi_h), \quad \forall \chi_h \in X_h.$$

This induces the discrete Green operator $G_h : X_h \rightarrow X_h$.

To state our approximation of the trilinear form b , we need more notation. Let $P_i, P_j \in \mathcal{P}_h$. If $P_i \neq P_j$ and they share an edge, we set:

$$\begin{aligned} S_h^{ij} &= \{J \in \mathcal{T}_h \mid P_i, P_j \in J\}; \\ \Gamma_{ij} &= \partial D_i \cap \partial D_j; \text{ and} \\ \nu_{ij} &= \text{the outer unit normal vector to } \Gamma_{ij}, \text{ outgoing from } D_i. \end{aligned}$$

Otherwise, we set $S_h^{ij} = \emptyset$, $\Gamma_{ij} = \emptyset$ and $\nu_{ij} = 0$. Restrictions of Γ_{ij} and ν_{ij} on $J \in S_h^{ij}$ are denoted by Γ_{ij}^J and ν_{ij}^J , respectively. Then we introduce the functionals β_{ij}^\pm on X_h by

$$\beta_{ij}^\pm(w_h) = \int_{\Gamma_{ij}} [\nabla G_h w_h \cdot \nu_{ij}]_\pm dS = \sum_{J \in S_h^{ij}} \text{meas}(\Gamma_{ij}^J) [(\nabla G_h w_h)_J \cdot \nu_{ij}^J]_\pm,$$

where $[a]_\pm = \max\{0, \pm a\}$ and $\text{meas}(\Gamma_{ij}^J) = \text{meas}_d(\Gamma_{ij}^J)$ is the d -dimensional Lebesgue measure. At this stage, writing

$$\Lambda_i = \{P_j \in \mathcal{P}_h \mid S_h^{ij} \neq \emptyset\},$$

we introduce a trilinear form b_h on $X_h \times X_h \times X_h$ by

$$b_h(w_h, u_h, \chi_h) = \sum_{i=1}^N \chi_h(P_i) \sum_{j \in \Lambda_i} \{u_h(P_i) \beta_{ij}^+(w_h) - u_h(P_j) \beta_{ij}^-(w_h)\}.$$

This is a direct application of Baba and Tabata's scheme [1]; see [6]. Finally, we introduce the backward Euler difference quotient by setting

$$\partial_{\tau_n} w_h^n = \frac{w_h^n - w_h^{n-1}}{\tau_n}, \quad (\{w_h^n\}_{n \geq 1} \subset X_h).$$

Now we can state our finite element scheme to (18): Find $\{u_h^n\}_{n \geq 0} \subset X_h$ such that

$$\begin{aligned} (\partial_{\tau_n} u_h^n, \chi_h)_h + (\nabla u_h^n, \nabla \chi_h) + b_h(u_h^{n-1}, u_h^n, \chi_h) &= 0, \quad \forall \chi_h \in X_h, \quad \forall n \geq 1 \\ u_h^0 &= u_{0h}, \end{aligned} \tag{19}$$

where $u_{0h} \in X_h$ is a suitable approximation of u_0 .

Remark 5.1. The first equality of (19) includes two linear systems. Thus, at each time step, we initially solve a linear system for $G_h u_h^{n-1}$ and then that of u_h^n . We note that $G_h u_h^n$ is an approximation of $v(t_n) = Gu(t_n)$.

We obtain mass conservation in this scheme.

Theorem 5.1. *Let $\{u_h^n\}_{n \geq 0} \subset X_h$ be a solution of (19). Then*

$$(u_h^n, 1)_h = (u_{0h}, 1)_h \tag{20}$$

for $n \geq 0$.

To proceed to the well-posedness and positivity conservation, we put

$$\kappa_h = \min_{J \in \mathcal{T}_h} \kappa_J, \quad (\kappa_J = \text{the minimal perpendicular length of } J)$$

and assume the acuteness.

(H1) It holds that

$$\max\{\cos(\nabla\phi_i^J, \nabla\phi_j^J) \mid 1 \leq i, j \leq d+1\} \leq 0, \quad \forall J \in \mathcal{T}_h \in \{\mathcal{T}_h\},$$

where $\{\phi_i^J\}_{i=1}^{d+1}$ represents the barycentric coordinates of J with respect to the vertices of J .

Remark 5.2. For $d = 2$, (H1) is equivalent to a statement that each triangle of \mathcal{T}_h is a right or an acute triangle. For $d = 3$, (H1) is satisfied if and only if all angles made by two faces of each tetrahedron of \mathcal{T}_h are less than or equal to $\pi/2$.

Theorem 5.2. *We assume (H1) and $u_{0h} \in X_h \geq 0, \neq 0$, and take $\tau > 0$ and $\varepsilon \in (0, 1]$. Then, (19) with a time step-size control*

$$\tau_n = \min \left\{ \tau, \frac{3(d-1)\varepsilon\kappa_h}{d^2(d+1)\|\nabla G_h u_h^{n-1}\|_\infty} \right\}$$

admits a unique solution $\{u_h^n\}_{n \geq 0} \subset X_h$ such that $u_h^n > 0$ for $n \geq 1$.

Combining this with Theorem 5.1, we immediately obtain

Corollary 5.1. *Let $\{u_h^n\}_{n \geq 0} \subset X_h$ be a solution of (19) as in Theorem 5.2. Then,*

$$\|u_h^n\|_1 = \|u_{0h}\|_1$$

for $n \geq 0$.

Remark 5.3. Because all norms are equivalent on X_h , we have

$$\|\nabla G_h u_h^{n-1}\|_\infty \leq c_h \|u_{0h}\|_1,$$

where c_h is a positive constants depending on h . Therefore, there is a $c'_h > 0$ such that $\tau_n \geq \min\{\tau, c'_h\}$. Thus τ_n never converges to zero as n increases; the algorithm always works. Consequently, u_h^n actually exists for all $n \geq 1$.

To derive convergence, we require the inverse assumption and elliptic regularity.

(H2) There exists a positive constant γ_2 such that

$$\gamma_2 h \leq h_J, \quad \forall J \in \mathcal{T}_h \in \{\mathcal{T}_h\}.$$

(R) There exists $\sigma \in (d, \infty)$ such that the following holds true: For any $p \in (1, \sigma)$ and $f \in L^p(\Omega)$, a linear elliptic problem

$$-\Delta v + v = f \quad \text{in } \Omega, \quad \frac{\partial v}{\partial \nu} = 0 \quad \text{on } \partial\Omega \quad (21)$$

admits a unique solution $v \in \mathcal{W}_p$ that satisfies

$$\|v\|_{2,p} \leq C \|f\|_p \quad (22)$$

with a constant $C = C(p, \Omega) > 0$.

Remark 5.4. When $\Omega \subset \mathbb{R}^2$ is a convex polygon, (R) is always satisfied. On the other hand, when $\Omega \subset \mathbb{R}^3$ is a convex polyhedron, it is satisfied, if all edges and all vertices of Ω are sufficiently small. For complete descriptions, see Theorems 8.2.1.2 and 8.2.2.8 of [2].

Theorem 5.3. *Suppose (H1), (H2), and (R), and assume a unique solution to (18) satisfying*

$$u \in C((0, T) : \mathcal{W}_p), \quad u' \in C((0, T) : W^{1,p}) \cap C^q((0, T) : L^p)$$

for some $p \in (d, \sigma)$ and $q \in (0, 1]$. Moreover, chose $u_{0h} \in X_h$

$$\|u_0 - u_{0h}\|_p \leq \alpha_{0,p} h^{1-d/p}, \quad (23)$$

with some $\alpha_{0,p} = \alpha_{0,p}(u_0) > 0$. Then, there exist positive constants h_0, τ_0 depending on $\Omega, T, p, q, \gamma_i$'s and u such that we have the error estimates

$$\sup_{0 \leq n \leq l} \|u(t_n) - u_h^n\|_p \leq C_1 (h^{1-d/p} + \tau^q), \quad (24)$$

$$\sup_{0 \leq n \leq l} \|Gu(t_n) - G_h u_h^n\|_{1,\infty} \leq C_2 (h^{1-d/p} + \tau^q) \quad (25)$$

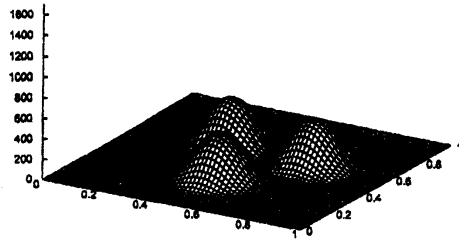
for $h \in (0, h_0)$ and $\tau \in (0, \tau_0)$, where $l = l(\tau, h) = \max\{n \in \mathbb{N} \mid t_n < J\}$, $\{u_h^n\}_{n \geq 0} \subset X_h$ is the solution of (19) as in Theorem 5.2.

Remark 5.5. In our scheme, the point-wise value of ∇v_h^{n-1} is used to determine the upwind nodal points at t_n . Thus, we need the estimate $v_h^n - v(t_n)$ in $W^{1,\infty}(\Omega)$ norm uniformly in t_n .

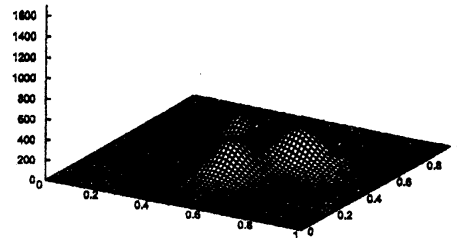
Figure 4 shows an example of numerical computation at several time levels t_n with the value of $\|u_h^n\|_1$. We assume that $\Omega = (0, 1)^2 \subset \mathbb{R}^2$ is a unit square and take \mathcal{T}_h as a uniform mesh composed of $2\ell^2$ equal right triangles for $\ell \in \mathbb{N}$; each side of Ω is divided into ℓ intervals of the same length. Then each small square is decomposed into two equal triangles by a diagonal. We note $h = \sqrt{2}\ell^{-1}$. We take $\mu = 1$ and $\varepsilon = 0.9$, and then highly concentrated solution is captured. Mass conservation is also confirmed. In Figure 5, we plot (t_n, τ_n) . We see that the more is concentrated the approximate solution, the smaller is τ_n .

6 Discussion

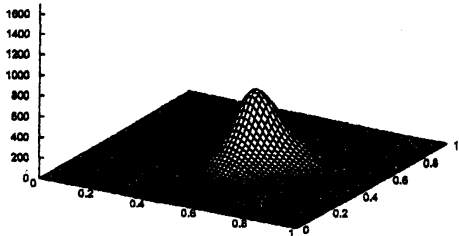
These numerical results are not reliable for $t \gg 1$. Actually, we have constructed numerical schemes so that the discrete solution preserves L^1 norm. Consequently, the discrete solution exists globally in time, because X_h is of finite-dimensional. Thus, we cannot look at the moment of blowup numerically. Also, structure of the total set of stationary solutions loses the fundamental profile of quantized blowup mechanism by discretization, and even nearly blowup discretized solution cannot describe this property. We have several more important profiles of the original solution from the viewpoint of self-organization; blowup rate, free energy transmission, and so forth, but we have not been able to realize them numerically also. Thus, Theorem 5.3 is not satisfactory, because it is valid only by the blowup time of u , which we are required to detect by the numerical computation. Still, we have a fruitful interaction between numerical computation and theoretical study concerning the movement of collapse formed on the boundary. See [10].



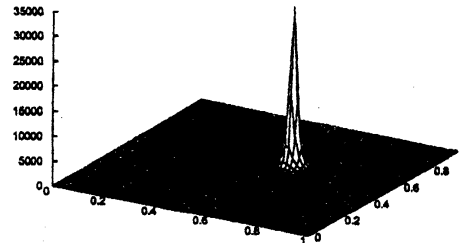
(i) $t_0 = 0.000000$
 $(\|u_{0h}\|_1 = 50.000)$



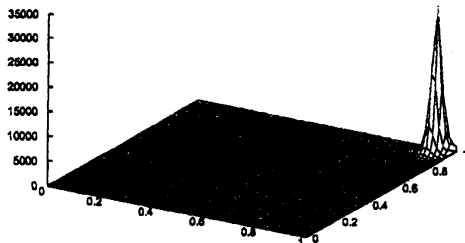
(ii) $t_n = 0.004538$
 $(\|u_h^n\|_1 = 50.000)$



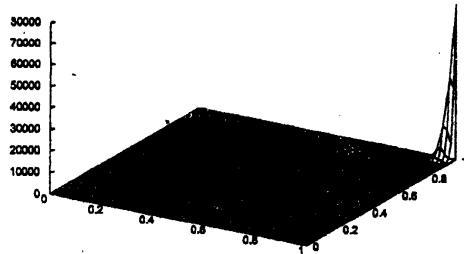
(iii) $t_n = 0.008587$
 $(\|u_h^n\|_1 = 50.000)$



(iv) $t_n = 0.045250$
 $(\|u_h^n\|_1 = 50.000)$



(v) $t_n = 0.089382$
 $(\|u_h^n\|_1 = 50.000)$



(vi) $t_n = 0.089635$
 $(\|u_h^n\|_1 = 50.000)$

Figure 4: Shape of u_h^n ($\mu = 1$; $\varepsilon = 0.9$; $\tau = h/2$; $\ell = 64$): (i), the initial function has three peaks; (ii)(iii)(iv), they gather and produce a peak; (v)(vi), the peak moves toward a corner.

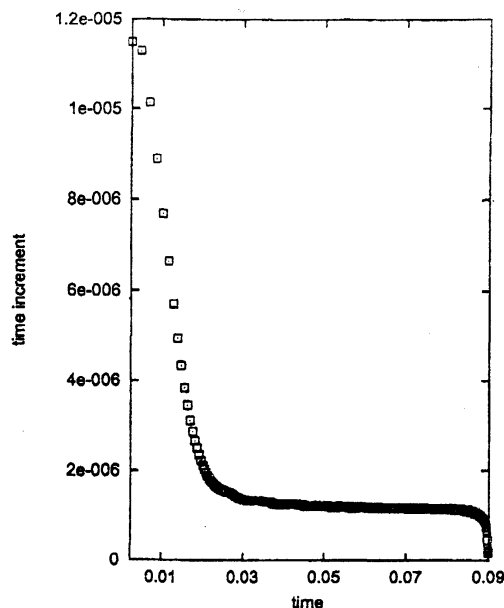


Figure 5: Time t_n versus time increment τ_n . ($0 < t_n < 0.09$; $\mu = 1$; $\varepsilon = 0.9$; $\tau = h/2$; $\ell = 64$; $\|u_{0h}\|_1 = 50.0$ and u_{0h} is illustrated in Fig. 4.)

References

- [1] K. Baba and M. Tabata: *On a conservative upwind finite element scheme for convective diffusion equations*, RAIRO Anal. Numér. **15** (1981) 3–25.
- [2] P. Grisvard: *Elliptic Problems in Nonsmooth Domains*, Boston, Pitman, 1983.
- [3] T. Hillen and H.G. Othmer: *The diffusion limit of transport equations derived from velocity jump processes*, SIAM J. Appl. Math. **61** (2000) 751–775.
- [4] E. F. Keller and L. A. Segel: *Initiation on slime mold aggregation viewed as instability*, J. Theor. Biol. **26** (1970) 399–415.
- [5] H. G. Othmer and A. Stevens: *Aggregation, blowup, and collapse: the ABCs of taxis in reinforced random walks*, SIAM J. Appl. Math. **57** (1997) 1044–1081.
- [6] N. Saito: *Conservative upwind finite element method for a simplified Keller-Segel system modelling chemotaxis*, submitted.
- [7] N. Saito and T. Suzuki: *Notes on finite difference schemes to a parabolic-elliptic system modelling chemotaxis*, Appl. Math. Comput. **171** (2005) 72–90.
- [8] A. Stevens: *The derivation of chemotaxis equations as limit dynamics of moderately interacting stochastic many-particle systems*, SIAM J. Appl. Math. **61** (2000) 183–212.
- [9] T. Suzuki: *Free Energy and Self-Interacting Particles*, Birkhäuser, Boston, 2005.

- [10] T. Suzuki: Mean Field Theories and Dual Variation, Elsevier, Amsterdam, 2006 (to be published).
- [11] M. Tabata: *A finite difference approach to the number of peaks of solutions for semilinear parabolic problems*, J. Math. Soc. Japan **32** (1980) 171-192.